

# Resveratrol Prevents Skeletal Muscle Atrophy and Senescence via Regulation of Histone Deacetylase 2 in Cigarette Smoke-Induced Mice with Emphysema

Chao Li<sup>1,\*</sup>, ZhaoHui Deng<sup>2,3,\*</sup>, GuiXian Zheng<sup>3,\*</sup>, Ting Xie<sup>3</sup>, XinYan Wei<sup>3</sup>, ZengYu Huo<sup>3</sup>, Jing Bai<sup>3</sup> 

<sup>1</sup>Department of Respiratory Medicine, Hunan Provincial People's Hospital, Changsha, Hunan, 410219, People's Republic of China; <sup>2</sup>Zhuzhou Hospital Affiliated to Xiangya School of Medicine, Zhuzhou, Hunan, 412000, People's Republic of China; <sup>3</sup>Department of Respiratory Medicine, the First Affiliated Hospital of Guangxi Medical University, Nanning, Guangxi, 530021, People's Republic of China

\*These authors contributed equally to this work

Correspondence: Jing Bai, Department of Respiratory Medicine, the First Affiliated Hospital of Guangxi Medical University, No. 6 Shuangyong Road, Nanning, Guangxi, Tel +86-771-5356702, Fax +86-771-5608132, Email bj1312002@aliyun.com

**Objective:** The aim of this study was to investigate the effects of resveratrol (RSV) on cigarette smoke (CS)-induced skeletal muscle atrophy and senescence in mice with emphysema and to explore the underlying mechanisms.

**Methods:** Gastrocnemius muscle weight and lung and muscular morphology were observed in CS-exposed mice with or without RSV treatment. The expression of atrophy-related markers (MURF1 and MAFbx), senescence-related markers (P53, P21 and SMP30) and NF- $\kappa$ B inflammatory pathways was detected by Western blotting and real-time PCR. The levels of IL-1 $\beta$  and TNF- $\alpha$  were also determined by ELISA, and the number of senescent cells was determined by SA- $\beta$  gal staining. In addition, the expression of HDAC2 and the effect of HDAC2 on CSE-induced skeletal muscle atrophy and senescence by RSV treatment were investigated.

**Results:** RSV prevented emphysema and skeletal muscle atrophy in long-term CS-exposed mice. RSV decreased the expression of MURF1, MAFbx, P53, and P21 and inhibited the NF- $\kappa$ B pathway both in vivo and in vitro. Moreover, RSV reversed CS-induced downregulation of HDAC2 expression both in gastrocnemius and in C2C12 cells. Moreover, knockdown of HDAC2 significantly abolished the inhibitory effect of RSV on the expression of MURF1, MAFbx, P53, P21 and inflammatory factors (IL-1 $\beta$  and TNF- $\alpha$ ) in C2C12 cells.

**Conclusion:** RSV prevents CS-induced skeletal muscle atrophy and senescence, and upregulation of HDAC2 expression and suppression of inflammation are involved.

**Keywords:** resveratrol, skeletal muscle, histone deacetylase 2, cigarette smoke, inflammation

## Introduction

Chronic obstructive pulmonary disease (COPD) is a highly prevalent respiratory disease that has significant morbidity and mortality worldwide.<sup>1</sup> It is characterized by incompletely reversible progressive airflow limitation and causes systemic multisystem damage.<sup>2,3</sup> The most important complications of COPD are skeletal muscle atrophy and dysfunction, which occur in the early stages of COPD and have been used to assess patients' quality of life and progression of disease.<sup>4-6</sup> Evidence suggests that the inflammatory response to cigarette smoke (CS) is the most important feature of COPD.<sup>7</sup> While it is associated with skeletal muscle atrophy,<sup>8</sup> it is also the main cause of skeletal muscle senescence.<sup>9</sup> Therefore, understanding the pathophysiology of this process will help to develop new therapies.

Skeletal muscle atrophy is closely related to reduced synthesis or increased breakdown of muscle proteins,<sup>5</sup> and the ubiquitin proteasome system (UPS) plays an essential role.<sup>10,11</sup> The E3 ligase muscle ring finger gene 1 (MURF1) and the muscle atrophy F-box (MAFbx) are key molecules in the UPS; both are predominantly expressed in muscle tissue,

and their expression levels are high in the quadriceps muscle of COPD patients.<sup>12–14</sup> Furthermore, cellular senescence occurs concomitantly in COPD.<sup>15</sup> It has been found that telomere maximum length is significantly reduced,<sup>16</sup> which is accompanied by DNA damage and activation of P53 and P21 in the muscles of COPD patients; these changes result in cell cycle arrest.<sup>17</sup> Interestingly, our previous study found that CS-induced skeletal muscle atrophy and senescence were associated with histone deacetylase 2 (HDAC2).<sup>18</sup> Other studies have found a significant decrease in HDAC2 expression in the quadriceps muscle of COPD patients, and it was positively correlated with FEV1% predicted and quadriceps maximum voluntary contraction force (MVC).<sup>19</sup> These results strongly highlight the importance of HDAC2 in the pathogenesis of COPD.

Resveratrol (RSV) is a natural polyphenolic compound with anti-inflammatory, antioxidant, anti-senescence and antitumor effects.<sup>20–23</sup> Previous studies have found that RSV decreases the levels of TNF- and increases the expression of SIRT1 to activate the AMPK pathway to improve muscle atrophy in COPD.<sup>24</sup> In addition, there may be a positive effect of RSV on skeletal muscle mitochondrial function in COPD patients.<sup>25</sup> However, whether RSV can prevent CS-induced skeletal muscle atrophy and senescence via HDAC2 has not been reported.

In the present study, we investigated the effects of RSV on CS-induced skeletal muscle atrophy and senescence *in vivo* and *in vitro* and explored the possible molecular mechanisms.

## Materials and Methods

### Animals

Thirty-two male C57BL/6 mice (14±2 g, 5–6 weeks) were randomly divided into four groups: the control group (N), the resveratrol group (RSV), the emphysema group (COPD) and the treatment group (C+RSV). The animals were obtained from the Animal Experimental of Guangxi Medical University, China. The N and RSV groups (n=8) were exposed to room air for 24 weeks, and the COPD and C+RSV groups (n=8) were exposed to cigarette smoke for 24 weeks, according to a previous report.<sup>18,26</sup> The RSV and C+RSV groups were treated with RSV (200 mg/kg, Sigma–Aldrich, USA) by gavage daily from week 25 through week 28, while the N and COPD groups were treated with an equivalent volume of saline from week 25 through week 28.

At the end of the experiment, the mice were sacrificed by exsanguination under anesthesia, and the gastrocnemius muscle was weighed. The right lung tissue and right gastrocnemius muscle were used for histological examination, and the other side of the gastrocnemius muscle was homogenized for further analysis, as previously described.<sup>18</sup>

### Histology

Lung tissue and gastrocnemius muscle were fixed in 10% formalin at room temperature overnight and paraffin-embedded. The tissue sections (4 µm) were stained with H&E staining and observed under a microscope (Olympus, Japan). The mean linear intercept of the alveolar space (MLI) and the cross-sectional area of the gastrocnemius muscle (CSA) were analyzed and quantified using a blinded method as previously described.<sup>18</sup>

### Cell Culture

Murine skeletal muscle C2C12 cells were obtained from the Type Culture Collection of the Chinese Academy of Sciences, Shanghai, China. The cells were maintained and cultured as previously described.<sup>18,26</sup> The differentiated cells were treated with 0.3% CSE or 50 µmol/L RSV (Sigma–Aldrich) for 24 hours or received a combination dose of both drugs.

### Cigarette Smoke Extract Preparation

Ten cigarettes were drawn with a syringe and shaken in 10 mL PBS in order to uniformly dissolve the smoke, and the cigarette smoke extract (CSE) was filtered twice through a 0.22-µm filter membrane (Millipore, USA). The CSE concentration was measured at 320 nm using a NanoDrop, and the CSE was diluted to a concentration that did not cause cell death. The working concentrations of CSE are based on the formulae reported in our previous studies.<sup>18</sup>

## Western Blot

Western blotting was used to verify the expressed proteins as previously described.<sup>18</sup> Briefly, gastrocnemius and C2C12 cells were lysed with RIPA buffer (Solarbio, Beijing, China), and protein was quantified by using a BCA protein assay kit (Beyotime, Shanghai, China). Forty micrograms of the samples were separated on 10–12% SDS-polyacrylamide gels and electrophoretically transferred onto PVDF membranes (Millipore, USA). After blocking with 5% fat-free milk in Tris-buffered saline (TBS) for 1 hour, the membranes were incubated with primary antibodies against HDAC2, P53, P21, IKK, NF- $\kappa$ Bp65 (all 1:1000, Cell Signaling Technology, USA), MURF1, MAFbx, and SMP30 (all 1:1000, Abcam, UK) overnight at 4 °C overnight, followed by incubation with fluorescent secondary antibodies (1:1000, Cell Signaling Technology, USA) for 1 hour. Quantification of signal intensities was quantified using ImageJ software.

## Real-Time PCR

Real-time PCR assays were performed as previously described.<sup>18</sup> Briefly, total RNA was extracted with TRIzol reagent (Invitrogen) and reverse-transcribed into cDNA using a reverse transcription kit (Promega, USA). Quantitative real-time PCR was performed using a SYBR<sup>®</sup> Premix Ex Taq II kit (Takara, Japan). The relative gene expression was calculated using the  $2^{-\Delta\Delta CT}$  method, and GAPDH was used as a reference. The PCR primers are shown in Table 1.

## ELISA

The levels of IL-1 and TNF- $\alpha$  in gastrocnemius muscle and cell supernatants were detected in triplicate using mouse ELISA kits according to the manufacturer's instructions (Cloud-Clone, Wuhan, China).

## CCK8 Assay

Cytotoxicity was monitored with a CCK8 kit (Dojindo, Shanghai, China). C2C12 cells ( $1 \times 10^4$  cells/well) were seeded into 96-well plates and pretreated with various concentrations of RSV for 24 hours. Then, CCK8 reagent was added to the plates, and the absorbance at 450 nm was recorded using a microplate reader (Biotek, Winooski, VT, USA). Four replicate wells were prepared for each concentration, and three independent experiments were performed to assess cellular viability.

**Table 1** The Sequences of RT-PCR Primers

HDAC2: forward (5'- AGCCCATGGCGTACAGTCAA-3')
Reverse (5'-GGGATGACCCTGGCCATAATAA-3')
MURF1: forward (5'- ATCACGCAGGAGCAGGAGGAG-3')
Reverse (5'-CTTGGCACTTGAGAGGAAGGTAGC-3')
MAFbx: forward (5'-TTCACAAAGGAAGTACGAAGGA-3')
Reverse (5'-GCTGGTCTTCAAGAACTTTCAG-3')
P53: forward (5'-TGGAAGGAAATTTGTATCCCGA-3')
Reverse (5'-GTGGATGGTGGTATACTCAGAG-3')
P21: forward (5'-ATGTCCAATCCTGGTGATGTC-3')
Reverse (5'-GAAGTCAAAGTTCCACCGTTC-3')
GAPDH: forward (5'- TGTGTCCGTCGTGGATCTGA-3')
Reverse (5'- TTGCTGTTGAAGTCGCAGGAG-3')

## Transfection of siRNA

Lentivirus synthesis and design were prepared by GeneChem (Shanghai, China). The C2C12 cell suspension was seeded into six-well plates at  $3 \times 10^5$  cells/well and incubated in 10% FBS DMEM at 37 °C until 30% confluence was reached. The lentiviruses were transfected into C2C12 cells at an MOI of 50 according to the manufacturer's instructions. The siRNA sequences were as follows: siRNA HDAC2-1: 5'-AGCATCAGACAAACGGATA-3', siRNA HDAC2-2: 5'-CAATGAGTTGCCATATAAT-3', siRNA HDAC2-3: 5'-ATCAATAAGACCAGATAAT-3'. Stably transduced cells were selected with puromycin (0.5 µg/mL) for 2 weeks. Then, the cells were pretreated with or without RSV for 24 hours and incubated with 0.3% CSE for 24 hours. Supernatants and cells were subjected to further analysis.

## Immunofluorescence Staining

Immunofluorescence and myotube analysis were performed as described previously.<sup>18</sup> Briefly, the differentiated C2C12 cells were fixed in 4% paraformaldehyde and stained with primary anti-MHC antibodies (1:200, Santa Cruz, USA) followed by fluorescent mouse antibodies (1:250, Cell Signaling Technology, USA). The samples were stained with DAPI (Solarbio, Beijing, China). All images were observed on a fluorescence microscope (Olympus CKX53, Japan) and myotubular parameters were analyzed using ImageJ software.

## SA-β Gal Staining

SA-β-gal activity was measured using an SA-β-gal staining kit (GENMED, Shanghai, China). The C2C12 cells were fixed and then stained with SA-β-gal staining solution at 37 °C for 12 hours according to the manufacturer's instructions. Positive cells were stained blue under a light microscope (Olympus, Japan). The ratio of positive cells was defined by the number of blue cells divided by the total number of cells.

## Statistical Analysis

All data are expressed as the means ± SDs. Differences among groups were analyzed by ANOVA and a post hoc Tukey–Kramer test. A P value of < 0.05 was considered statistically significant.

## Results

### Resveratrol Ameliorates Emphysema and Skeletal Muscle Atrophy

To determine the effect of RSV on emphysema and gastrocnemius muscle in CS-exposed mice, the pathology of the lungs and skeletal muscles and the weight of the gastrocnemius muscle were assessed. Compared to the control group, CS-exposed mice exhibited significantly increased mean lining intercepts (MLIs) and reduced cross-sectional areas (CSAs) of the gastrocnemius muscle. Compared to the emphysema group, these parameters were improved in the treated group ( $P < 0.05$ ) (Figure 1A and B). In addition, there was no significant difference in body weight or gastrocnemius weight between the treatment and emphysema groups ( $P < 0.05$ ) (Figure 1C and D). These data suggest that RSV reverses the development of chronic CS-induced emphysema and skeletal muscle atrophy.

### Resveratrol Decreases Atrophy- and Senescence-Related Protein Expression in the Gastrocnemius Muscle

Compared to the control group, the expression of atrophy-related proteins (MURF1, MAFbx) and senescence-related proteins (P53, P21) was significantly increased, while SMP30 protein levels were significantly reduced in the gastrocnemius muscle of CS-exposed mice. Treatment with RSV reduced CS-induced increases in MURF1, MAFbx, P53, and P21 protein levels and increased SMP30 protein levels ( $P < 0.05$ ) (Figure 2A and B). Similar results were observed for the mRNA expression of MURF1, MAFbx, P53, and P21 in the gastrocnemius muscle of CS-exposed mice ( $P < 0.05$ ) (Figure 2C and D). These results suggest that RSV has anti-atrophy and anti-senescence effects in the gastrocnemius muscle of CS-exposed mice.



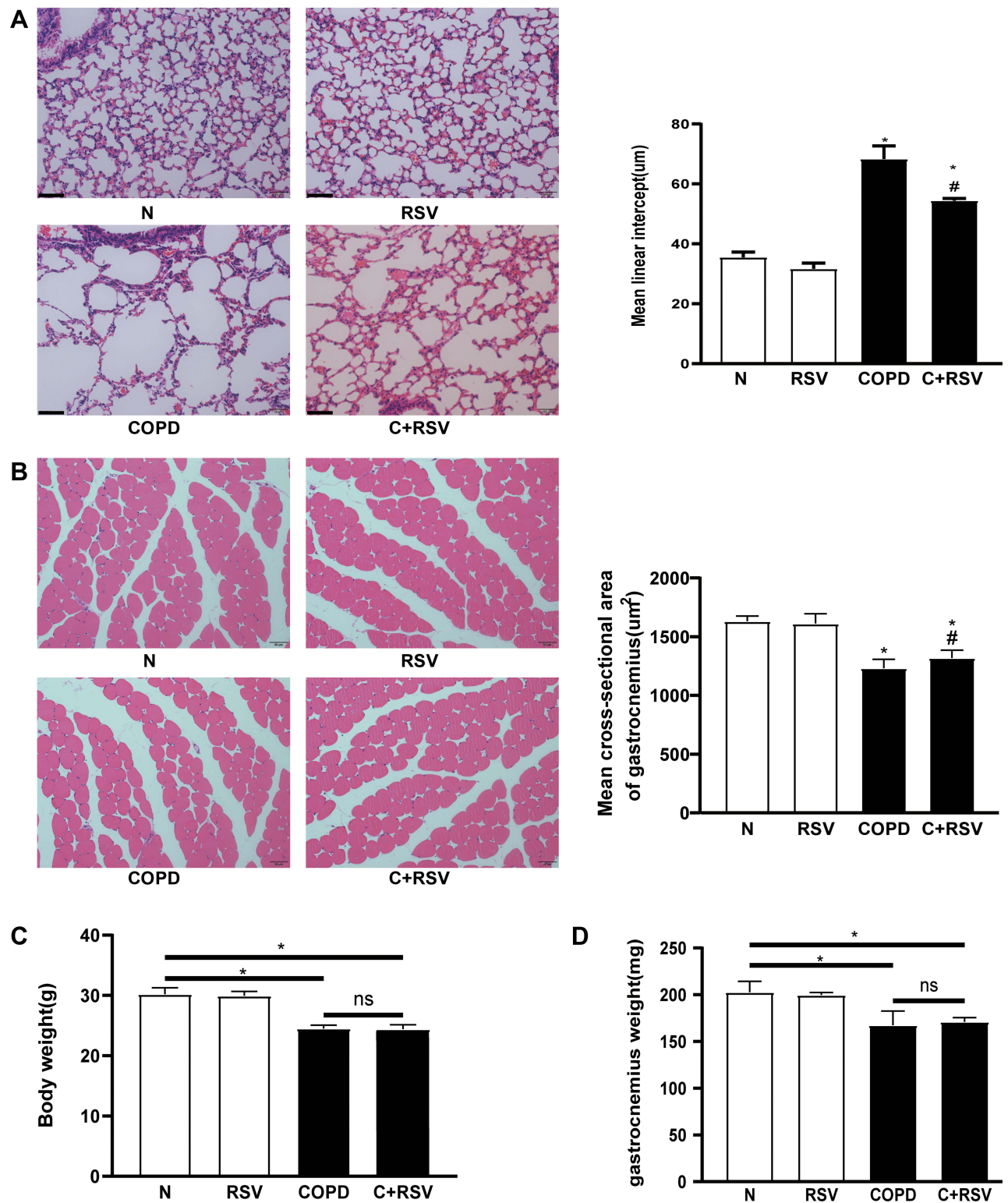


**Figure 1** Resveratrol prevents CS-induced emphysema and skeletal muscle atrophy in mice. **(A)** Representative lung tissue and gastrocnemius muscle. **(B)** H&E staining in mice exposed to CS for 24 weeks and treated with or without resveratrol (200 mg/kg) for 4 weeks. The mean lining intercept (MLI) and gastrocnemius cross-sectional area (CSA) of mice were calculated in each group. **(C)** Effect of resveratrol treatment on body weight and **(D)** weight of the gastrocnemius muscle. Data are representative images (magnification  $\times 200$ ) and expressed as the means $\pm$ SD of each group ( $n=8$ ) of mice. \* $p<0.05$  vs control group (N), # $p<0.05$  vs COPD.

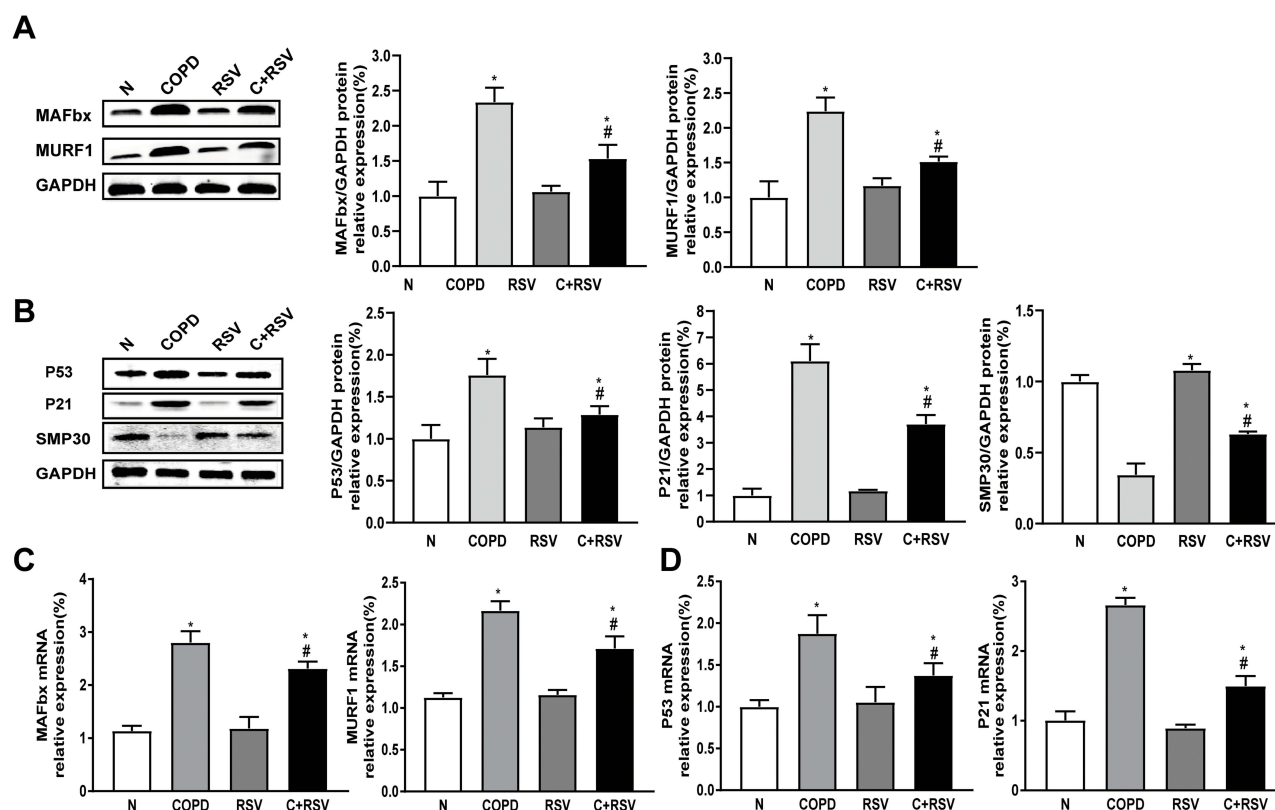


**Figure 2** Treatment with resveratrol reduces the expression of atrophy and senescence-related markers in the CS-induced gastrocnemius muscle of mice. Protein and mRNA were extracted from the gastrocnemius muscle for Western blot and RT-PCR analysis. (A) The expression levels of atrophy-associated proteins MURF1 and MAFbx and (C) their mRNA expression levels were examined in each group. (B) The expression levels of senescence-associated proteins P53, P21, and SMP30 and (D) their mRNA expression levels were examined in each group. GAPDH was used as the reference. Values are expressed as the means $\pm$ SDs. Three independent experiments were performed. \* $p$ <0.05 vs control group (N), # $p$ <0.05 vs COPD.

## Resveratrol Inhibits CSE-Induced Myotubular Atrophy in vitro

We examined the effect of RSV treatment on myotubular atrophy in C2C12 cells after incubation with 0.3% CSE for 24 hours. The data showed that the presence of RSV had no significant effect on the viability of C2C12 cells until the concentration of RSV increased to 100  $\mu$ mol/L, suggesting that low doses of RSV (<100  $\mu$ mol/L) had no significant cytotoxicity on C2C12 cells ( $P$ <0.05) (Figure 3A). Additionally, the CSE group exhibited a significant increase in mRNA and protein expression of MURF1 and MAFbx compared to the control group. Both the mRNA and protein levels of MURF1 and MAFbx were significantly decreased in C2C12 cells treated with RSV compared to the CSE group ( $P$ <0.05) (Figure 3B and C). Moreover, the CSE-induced myotube diameter of C2C12 cells was significantly smaller than that of the control group, while the CSE-induced myotube diameter decrease was reversed by RSV treatment ( $P$ <0.05) (Figure 3D).

## Resveratrol Ameliorates CSE-Induced Senescence in vitro

To further investigate the effect of RSV on CSE-induced cellular senescence, we also examined senescence-related phenotypes. As shown in Figure 4, the expression levels of P53 and P21 were significantly increased in the CSE group, and RSV inhibited P53 and P21 expression levels after incubation with CSE. In contrast, RSV treatment increased the protein expression of SMP30 in CSE-treated C2C12 cells ( $P$ <0.05) (Figure 4A and B). Furthermore, we found that the number of senescent cells in the CSE group was significantly increased compared to that in the control group. Treatment with RSV reduced the increase in CSE-induced senescence in C2C12 cells ( $P$ <0.05) (Figure 4C).

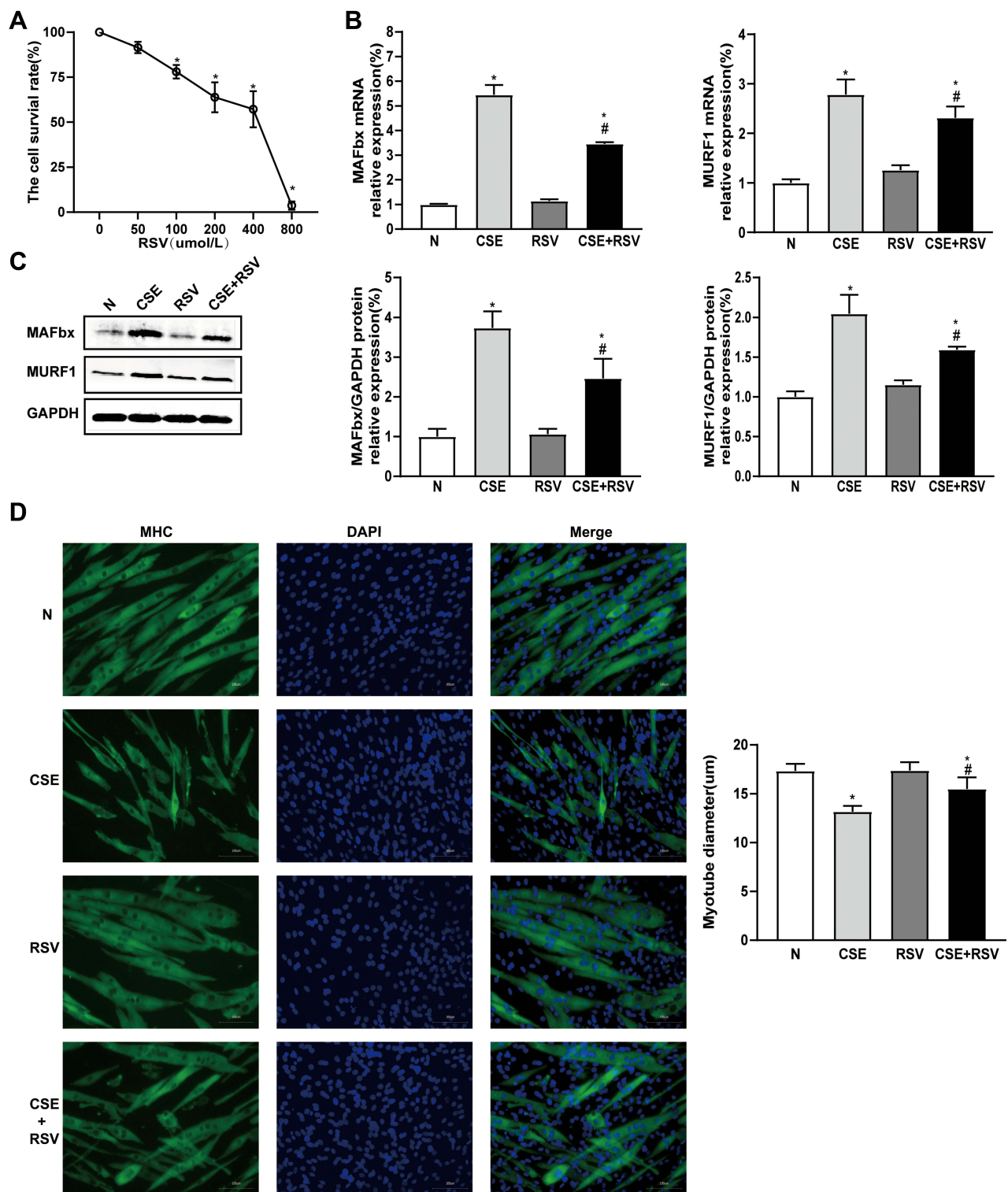


**Figure 3** Treatment with resveratrol inhibits CSE-induced atrophy in C2C12 cells. Cellular myotubes and atrophy-associated marker expression were determined after treatment with vehicle alone, resveratrol (50 μmol/L), 0.3% CSE, or a combination of 0.3% CSE and resveratrol (50 μmol/L). **(A)** The viability of C2C12 cells treated with increasing concentrations of RSV for 24 hours under normal conditions was assessed by CCK8 assay. \* $p < 0.05$  vs 0 μmol/L RSV. **(B)** The mRNA expression levels of MURF1 and MAFbx were examined by RT-PCR in each group, and **(C)** their protein expression levels were examined by Western blotting. GAPDH was used as the reference. **(D)** Photomicrographs of myotube cultures and quantification of the mean myotube diameter in each group (magnification  $\times 200$ ). Values are expressed as the means  $\pm$  SDs. Experiments were repeated 3 times independently. \* $p < 0.05$  vs control group (N), # $p < 0.05$  vs CSE.



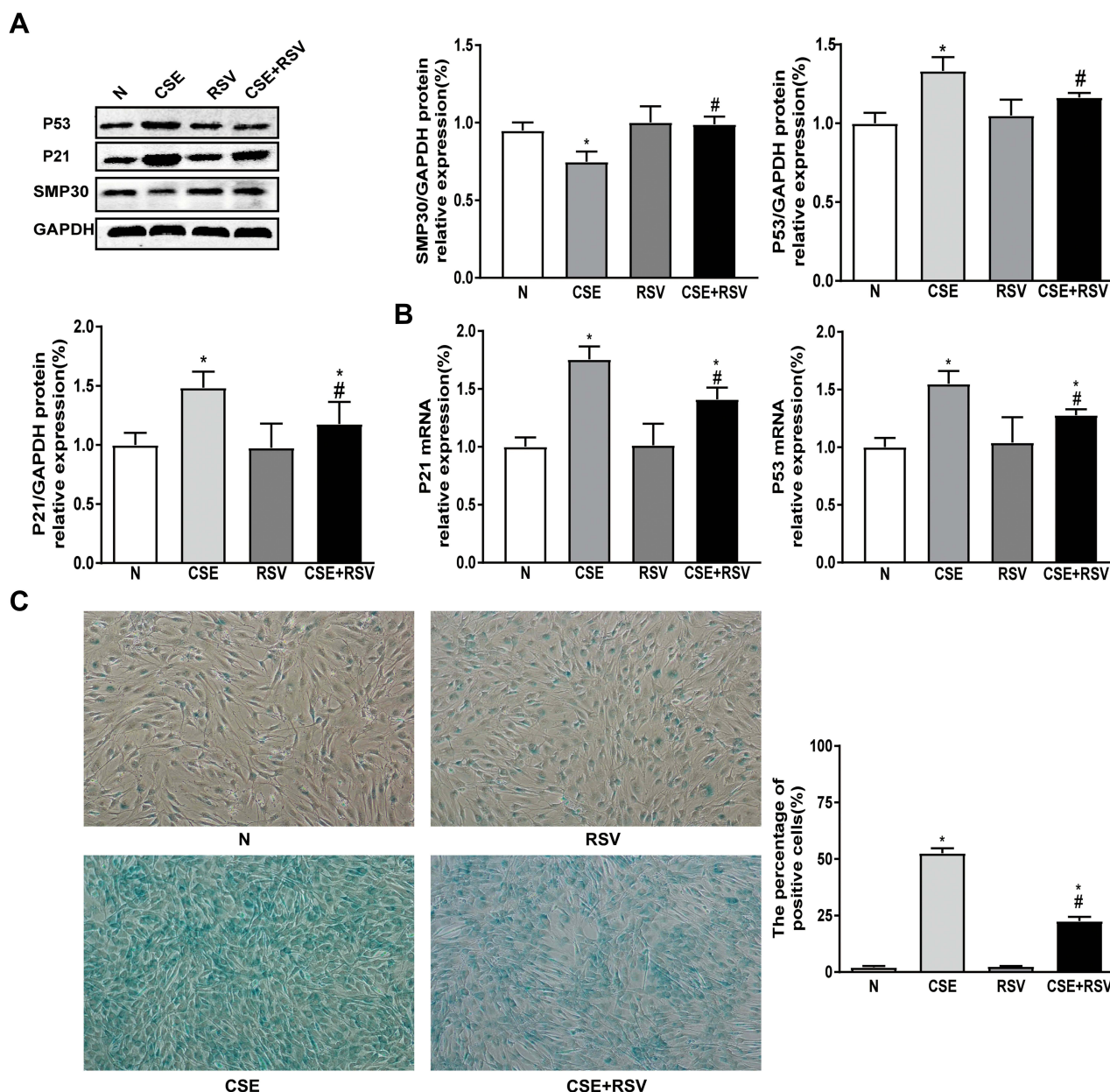


**Figure 4** Treatment with resveratrol inhibits CSE-induced senescence in C2C12 cells. Senescent cells and senescence-associated marker expression were determined after treatment with vehicle alone, resveratrol (50  $\mu\text{mol/L}$ ), 0.3% CSE, or a combination of 0.3% CSE and resveratrol (50  $\mu\text{mol/L}$ ). **(A)** The protein expression levels of P53, P21, and SMP30 were examined by Western blotting, and **(B)** their mRNA expression levels were examined by RT-PCR. GAPDH was used as the reference. **(C)** Cellular senescence of C2C12 cells was detected by  $\beta$ -galactosidase staining. Left: Representative images of C2C12 cell senescence in each group; Right: Quantification of senescent cells in each group (magnification  $\times 100$ ). Values are expressed as the means  $\pm$  SDs. Experiments were repeated 3 times independently. \* $p < 0.05$  vs control group (N), # $p < 0.05$  vs CSE.

## Resveratrol Increases HDAC2 Expression and Reduces Inflammation Both in vitro and in vivo

It has been demonstrated that CS-induced skeletal muscle atrophy and senescence are associated with the HDAC2-mediated inflammatory response.<sup>18,26</sup> We next investigated the effects of RSV on HDAC2 and inflammation levels in vivo and in vitro. Compared with the control group, the gastrocnemius muscle of CS-exposed mice showed significantly decreased HDAC2 mRNA and protein expression and increased IKK and NF- $\kappa$ B p65 protein levels. These effects were reversed by RSV ( $P < 0.05$ ) (Figure 5A-C). In addition, RSV inhibited the CS-induced increase in IL-1 $\beta$  and TNF- $\alpha$  levels ( $P < 0.05$ ) (Figure 5D).

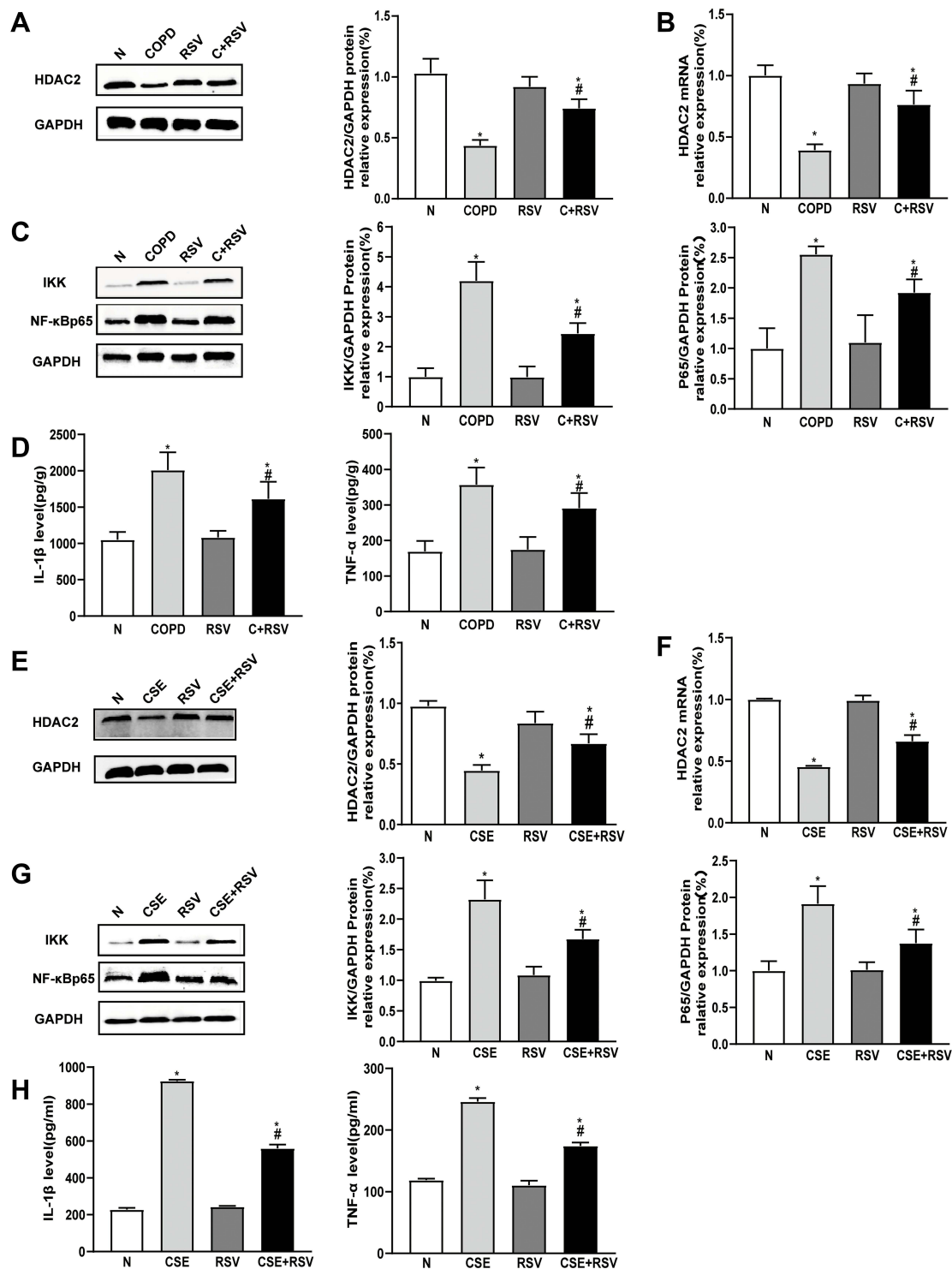


**Figure 5** Treatment with resveratrol increases HDAC2 expression and reduces inflammation in vivo and in vitro. **(A and B)** Mice were exposed to CS for 24 weeks and treated with or without resveratrol (200 mg/kg) for 4 weeks. Proteins and mRNA were extracted from the gastrocnemius muscle, and the expression of HDAC2 was measured by Western blot and RT-PCR. **(C)** The protein expression levels of IKK and NF-κBp65 were measured by Western blot. **(D)** IL-1β and TNF-α levels in mice were detected by ELISA. **(E and F)** C2C12 cells were pretreated with RSV (50 μmol/L), followed by incubation with 0.3% CSE for 24 hours. The expression of HDAC2 protein and mRNA was measured by Western blot and RT-PCR, **(G)** the protein expression levels of IKK and NF-κBp65 were measured by Western blot, and **(H)** IL-1β and TNF-α levels were detected by ELISA in C2C12 cells. GAPDH was used as the reference. Values are expressed as the means±SDs. Experiments were repeated 3 times independently. \*p<0.05 vs control group (N), #p<0.05 vs COPD or CSE.

As expected, the results showed that IL-1 $\beta$  and TNF- $\alpha$  levels were significantly higher after CSE incubation in C2C12 cells. In addition, C2C12 cells in the CSE group exhibited a significant decrease in both mRNA and protein expression of HDAC2 and a significant increase in protein expression of IKK and NF- $\kappa$ B p65 compared with the control group. However, RSV inhibited CSE-induced IL-1 $\beta$  and TNF- $\alpha$  levels, as well as the protein expression of IKK and NF- $\kappa$ B p65 in C2C12 cells ( $P < 0.05$ ) (Figure 5G and H). Moreover, RSV increased the mRNA and protein expression of HDAC2 ( $P < 0.05$ ) (Figure 5E and F). These findings demonstrated that RSV regulates HDAC2 and inflammation both in vivo and in vitro.

## Knockdown of HDAC2 Abrogates the Effect of Resveratrol on the Behavior of CSE-Exposed C2C12 Cells

To determine the role of HDAC2 in RSV protection against CSE-induced atrophy and senescence, HDAC2 was knocked down by transfection with siRNAs. As shown in Figure 6A, the mRNA and protein levels of HDAC2 were significantly reduced by lentiviral transduction of HDAC2 siRNA ( $P < 0.05$ ) (Figure 6A). Notably, HDAC2 knockdown significantly abolished RSV-mediated inhibition of CSE-induced atrophy (Figure 6B), senescence (Figure 6C) and inflammation ( $P < 0.05$ ) (Figure 6D) in C2C12 cells. These results suggest that RSV prevents skeletal muscle atrophy and senescence by regulating HDAC2 and suppressing inflammation.

## Discussion

Resveratrol (RSV) is a food-derived compound with anti-inflammatory, antioxidant, metabolic and cardioprotective potential. Recent clinical studies in non-COPD populations show improved mitochondrial oxidative metabolism after RSV treatment, which could be beneficial for both lung and muscle impairment in COPD. In the present study, we investigated the role of RSV in CS-induced skeletal muscle atrophy and senescence and the possible mechanisms. These results indicated that RSV ameliorates CS-induced skeletal muscle atrophy and senescence by upregulating HDAC2 and suppressing inflammation, which opens new prospects for further clinical treatment.

Currently, the development of COPD is associated with CS, which causes lung injury<sup>27</sup> and is also a common risk factor for skeletal muscle atrophy and dysfunction.<sup>4</sup> In recent years, MURF1 and MAFbx in the UPS have been shown to be involved in the regulation of muscle proteins.<sup>28</sup> In COPD, the expression of the E3 ligases MAFbx and Nedd4 is significantly increased in the quadriceps muscle.<sup>13</sup> Here, we found that CS significantly induced MURF1 and MAFbx protein expression in gastrocnemius and C2C12 cells. In addition, Saini<sup>29</sup> found that oxidative modification of muscle proteins by CSE can directly induce skeletal muscle cell senescence. The present study also demonstrated that the expression of P53 and P21 increased and the expression of SMP30 decreased after exposure to CS, which further supports previous findings.

The role of RSV in antioxidative stress, inhibiting NF- $\kappa$ B and activating AMPK has been demonstrated.<sup>30–33</sup> RSV inhibits dexamethasone-induced FOXO1 acetylation and MAFbx and MuRF1 expression and prevents protein degradation and myotubular atrophy in myoblasts.<sup>34</sup> Wang<sup>35</sup> also found a decrease in myotube diameter and an increase in MAFbx and MURF1 protein expression in C2C12 cells after TNF- $\alpha$  stimulation, while RSV reversed these changes via the Akt/mTOR/FoxO1 pathway. In this study, 200 mg/kg/d RSV was selected and then administered by gavage to emphysematous mice for 4 weeks, according to a previous report.<sup>36</sup> We examined pathological changes in the lung and gastrocnemius muscles as well as changes in the expression of atrophy- and senescence-associated proteins. The results showed that RSV treatment ameliorated the CS-induced significant increase in MLI and significant decrease in CSA while reversing the increased expression of MURF1 and MAFbx in the gastrocnemius muscle of mice. Similar results were observed in vitro. However, RSV failed to prevent the loss of body weight and gastrocnemius muscle weight in mice with emphysema, which may be associated with the short-term treatment duration of RSV. Furthermore, the anti-senescence effect of RSV was also reported.<sup>37,38</sup> We examined changes in the expression of senescence-associated proteins and found that RSV also inhibited the CS-induced increase in P53 and P21 protein expression and increased the expression levels of the senescence-associated protein SMP30. These results suggest that RSV prevents skeletal muscle atrophy and senescence in mice with emphysema.



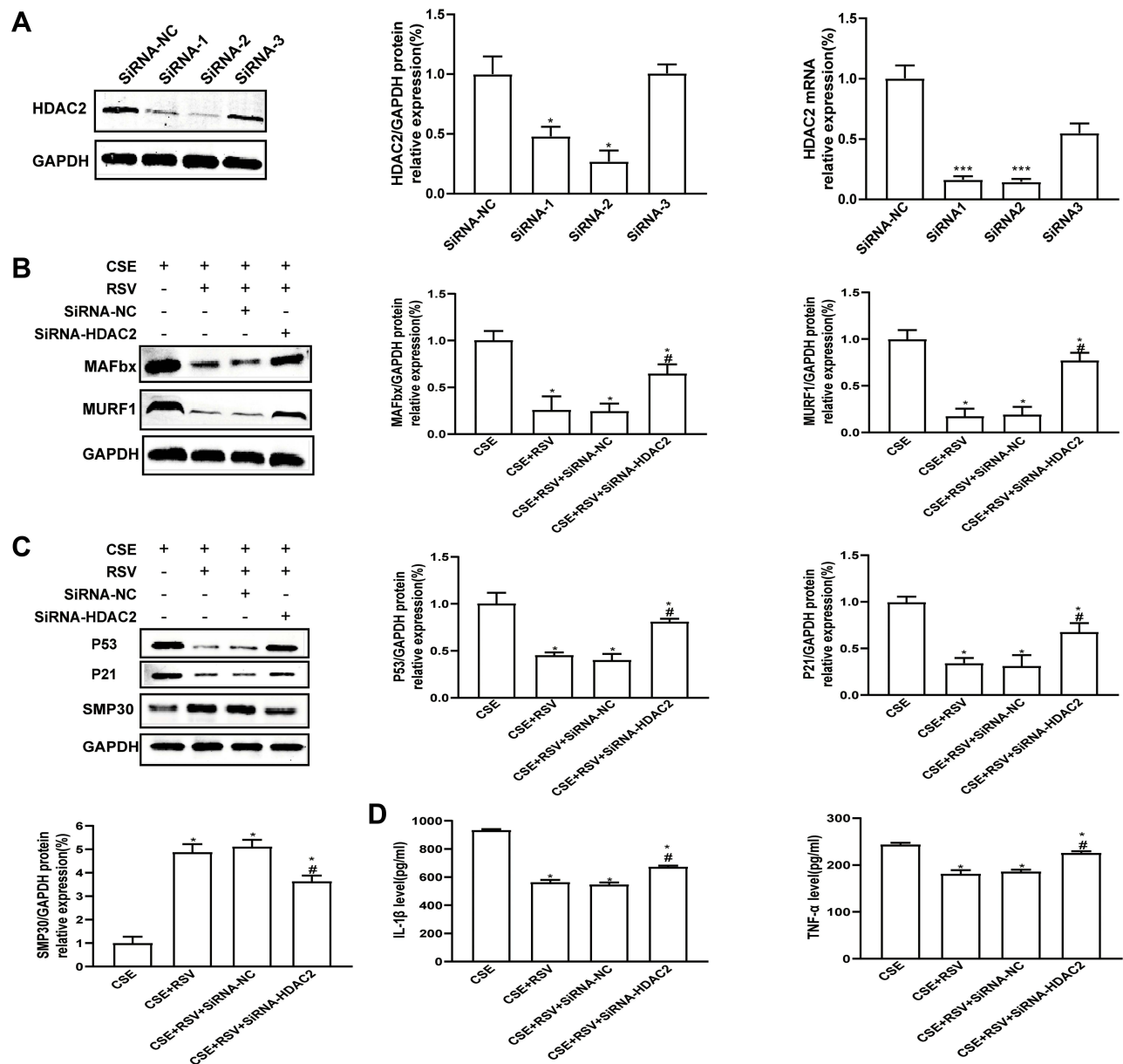


**Figure 6** Knockdown of HDAC2 abrogates the effect of resveratrol on the behavior of CSE-exposed C2C12 cells. **(A)** HDAC2 knockdown efficiency in C2C12 cells was validated by Western blot and RT-PCR. \* $p < 0.05$  vs siRNA-NC, \*\*\* $p < 0.01$  vs siRNA-NC. After lentiviral transfection, C2C12 cells were treated with 0.3% CSE or a combination of 0.3% CSE and resveratrol (50  $\mu\text{mol/L}$ ). **(B)** The protein expression levels of MURF1 and MAFbx and of **(C)** P53, P21, and SMP30 were examined by Western blotting. **(D)** The levels of IL-1 $\beta$  and TNF- $\alpha$  were detected by ELISA. GAPDH was used as the reference. Values are expressed as the means  $\pm$  SDs. Experiments were repeated 3 times independently. \* $p < 0.05$  vs CSE, # $p < 0.05$  vs CSE+RSV+siRNA-NC.

In addition, RSV treatment significantly decreased the protein expression of NF- $\kappa$ Bp65 and IKK, as well as the levels of TNF- $\alpha$  and IL-1 $\beta$ , in CS-exposed mice, suggesting the anti-inflammatory effect of RSV on skeletal muscle in COPD. Importantly, our previous study confirmed that HDAC2 is closely associated with CS-induced skeletal muscle atrophy and senescence.<sup>18</sup> In the present study, we found that RSV treatment inhibited the CS-induced decrease in the mRNA and protein expression of HDAC2 in vivo and in vitro. This effect may be associated with the suppression of CS-induced oxidative stress. To further explore the role of HDAC2 in RSV, we knocked down HDAC2 in C2C12 cells using lentivirus. Knockdown of HDAC2 partially abrogated RSV-mediated inhibition of CSE-induced skeletal muscle atrophy and senescence. Furthermore, inflammatory factors were consistent with the above phenotype, and

knockdown of HDAC2 caused increased IL-1 $\beta$  and TNF- $\alpha$  levels after RSV treatment. These results indicate that HDAC2 plays an important role in the prevention of CS-induced skeletal muscle atrophy and senescence by RSV.

The major limitations of this study are as follows: (1) RSV was used as an activator of SIRT1, and we did not investigate whether the protective effect of RSV on CS-induced skeletal muscle atrophy and senescence was involved in the activation of SIRT1; (2) HDAC2-knockout mice were established to investigate the role of HDAC2 in RSV-mediated inhibition of skeletal muscle atrophy and senescence in subsequent studies.

## Conclusion

In conclusion, RSV prevented CS-induced skeletal muscle atrophy and senescence in mice with emphysema. In addition, RSV inhibited CSE-induced myotubular atrophy and senescence in C2C12 cells. The mechanism may involve RSV-mediated upregulation of HDAC2 expression as well as inhibition of inflammation.

## Abbreviations

RSV, resveratrol; HDAC2, histone deacetylase 2; CSE, cigarette smoke extract; COPD, chronic obstructive pulmonary disease; MURF1, muscle ring finger gene 1; MAFbx, muscle atrophy F-box; SMP30, senescence marker protein-30.

## Ethics Approval and Consent to Participate

All animal experiments were conducted in accordance with the Guide for the Care and Use of Laboratory Animals and approved by the Institutional Animal Care Committee (IACUC), an organization accredited by the International Association for the Assessment and Accreditation of Laboratory Animal Care in China and the Guangxi Medical University Laboratory Animal Committee (No.201911013).

## Acknowledgments

This work was supported by the National Natural Science Foundation of China (81560008, 81960010), and Natural Science Foundation of Guangxi (2017GXNSFAA198130, 2018GXNSFAA050056, 2020GXNSFAA297143).

## Disclosure

The authors declare no conflict of interest.

## References

1. Singh D, Agusti A, Anzueto A, et al. Global Strategy for the Diagnosis, Management, and Prevention of Chronic Obstructive Lung Disease: the GOLD science committee report 2019. *Eur Respir J*. 2019;5:53.
2. Vanfleteren L, Spruit MA, Wouters EFM, Franssen FME. Management of chronic obstructive pulmonary disease beyond the lungs. *Lancet Respir Med*. 2016;4:911–924. doi:10.1016/S2213-2600(16)00097-7
3. Wang MT, Liou JT, Lin CW, et al. Association of Cardiovascular Risk With Inhaled Long-Acting Bronchodilators in Patients With Chronic Obstructive Pulmonary Disease: a Nested Case-Control Study. *JAMA Intern Med*. 2018;178:229–238. doi:10.1001/jamainternmed.2017.7720
4. Jaitovich A, Barreiro E. Skeletal Muscle Dysfunction in Chronic Obstructive Pulmonary Disease. What We Know and Can Do for Our Patients. *Am J Respir Crit Care Med*. 2018;198:175–186. doi:10.1164/rccm.201710-2140CI
5. Langen RC, Gosker HR, Remels AH, Schols AM. Triggers and mechanisms of skeletal muscle wasting in chronic obstructive pulmonary disease. *Int J Biochem Cell Biol*. 2013;45:2245–2256. doi:10.1016/j.biocel.2013.06.015
6. Kharbada KS, Ramakrishna A. Prevalence of quadriceps muscle weakness in patients with COPD and its association with disease severity. *Int J Chron Obstruct Pulmon Dis*. 2015;2:1727.
7. Barnes PJ. Oxidative stress-based therapeutics in COPD. *Redox Biol*. 2020;33:101544. doi:10.1016/j.redox.2020.101544
8. Degens H, Gayan-Ramirez G, Van Hees HWH. Smoking-induced Skeletal Muscle Dysfunction. From Evidence to Mechanisms. *Am J Respir Crit Care Med*. 2015;191:620–625. doi:10.1164/rccm.201410-1830PP
9. Barnes PJ. Senescence in COPD and Its Comorbidities. *Annu Rev Physiol*. 2017;79:517–539. doi:10.1146/annurev-physiol-022516-034314
10. Schiaffino S, Dyar KA, Ciciliot S, Blaauw B, Sandri M. Mechanisms regulating skeletal muscle growth and atrophy. *FEBS J*. 2013;280:4294–4314. doi:10.1111/febs.12253
11. Zheng N, Shabek N. Ubiquitin Ligases: structure, Function, and Regulation. *Annu Rev Biochem*. 2017;86:129–157. doi:10.1146/annurev-biochem-060815-014922
12. Rom O, Reznick AZ. The role of E3 ubiquitin-ligases MuRF-1 and MAFbx in loss of skeletal muscle mass. *Free Radic Biol Med*. 2016;98:218–230. doi:10.1016/j.freeradbiomed.2015.12.031
13. Plant PJ, Brooks D, Faughnan M, et al. Cellular markers of muscle atrophy in chronic obstructive pulmonary disease. *Am J Respir Cell Mol Biol*. 2010;42:461–471. doi:10.1165/rccm.2008-0382OC

14. Pomiès P, Blaquière M, Maury J, Mercier J, Gouzi F, Hayot M. Involvement of the FoxO1/MuRF1/Atrogin-1 Signaling Pathway in the Oxidative Stress-Induced Atrophy of Cultured Chronic Obstructive Pulmonary Disease Myotubes. *PLoS One*. 2016;11:e0160092. doi:10.1371/journal.pone.0160092
15. Mercado N, Ito K, Barnes PJ. Accelerated ageing of the lung in COPD: new concepts. *Thorax*. 2015;70:482–489. doi:10.1136/thoraxjnl-2014-206084
16. Thériault ME, Paré M, Maltais F, Debigaré R. Satellite cells senescence in limb muscle of severe patients with COPD. *PLoS One*. 2012;7:e39124. doi:10.1371/journal.pone.0039124
17. Barnes PJ, Baker J, Donnelly LE. Cellular Senescence as a Mechanism and Target in Chronic Lung Diseases. *Am J Respir Crit Care Med*. 2019;200:556–564. doi:10.1164/rccm.201810-1975TR
18. Li C, Deng Z, Zheng G, et al. Histone Deacetylase 2 Suppresses Skeletal Muscle Atrophy and Senescence via NF-κB Signaling Pathway in Cigarette Smoke-Induced Mice with Emphysema. *Int J Chron Obstruct Pulmon Dis*. 2021;16:1661–1675. doi:10.2147/COPD.S314640
19. To M, Swallow EB, Akashi K, et al. Reduced HDAC2 in skeletal muscle of COPD patients. *Respir Res*. 2017;18:99. doi:10.1186/s12931-017-0588-8
20. Malaguarnera L. Influence of Resveratrol on the Immune Response. *Nutrients*. 2019;11:545.
21. Vervandier-Fasseur D, Latruffe N. The Potential Use of Resveratrol for Cancer Prevention. *Molecules*. 2019;24:78.
22. Li YR, Li S, Lin CC. Effect of resveratrol and pterostilbene on aging and longevity. *Biofactors*. 2018;44:69–82. doi:10.1002/biof.1400
23. Wang XL, Li T, Li JH, Miao SY, Xiao XZ. The Effects of Resveratrol on Inflammation and Oxidative Stress in a Rat Model of Chronic Obstructive Pulmonary Disease. *Molecules*. 2017;22:326.
24. Qi Y, Shang JY, Ma LJ, et al. Inhibition of AMPK expression in skeletal muscle by systemic inflammation in COPD rats. *Respir Res*. 2014;15:156. doi:10.1186/s12931-014-0156-4
25. Beijers RJ, Gosker HR, Sanders KJ, et al. Resveratrol and metabolic health in COPD: a proof-of-concept randomized controlled trial. *Clin Nutr*. 2020;39:2989–2997. doi:10.1016/j.clnu.2020.01.002
26. Bin Y, Xiao Y, Huang D, et al. Theophylline inhibits cigarette smoke-induced inflammation in skeletal muscle by upregulating HDAC2 expression and decreasing NF-κB activation. *Am J Physiol Lung Cell Mol Physiol*. 2019;316:L197–L205. doi:10.1152/ajplung.00005.2018
27. Duffy SP, Criner GJ. Chronic Obstructive Pulmonary Disease: evaluation and Management. *Med Clin North Am*. 2019;103:453–461. doi:10.1016/j.mcna.2018.12.005
28. Foletta VC, White LJ, Larsen AE, Leger B, Russell AP. The role and regulation of MAFbx/atrogin-1 and MuRF1 in skeletal muscle atrophy. *Pflugers Arch*. 2011;461:325–335. doi:10.1007/s00424-010-0919-9
29. Saini A, Mastana S, Myers F, Lewis MP. ‘From death, lead me to immortality’ - mantra of ageing skeletal muscle. *Curr Genomics*. 2013;14:256–267. doi:10.2174/1389202911314040004
30. Burns J, Yokota T, Ashihara H, Lean ME, Crozier A. Plant foods and herbal sources of resveratrol. *J Agric Food Chem*. 2002;50:3337–3340. doi:10.1021/jf0112973
31. Borra MT, Smith BC, Denu JM. Mechanism of human SIRT1 activation by resveratrol. *J Biol Chem*. 2005;280:17187–17195. doi:10.1074/jbc.M501250200
32. Jackson JR, Ryan MJ, Hao Y, Alway SE. Mediation of endogenous antioxidant enzymes and apoptotic signaling by resveratrol following muscle disuse in the gastrocnemius muscles of young and old rats. *Am J Physiol Regul Integr Comp Physiol*. 2010;299:R1572–R1581. doi:10.1152/ajpregu.00489.2010
33. Centeno-Baez C, Dallaire P, Marette A. Resveratrol inhibition of inducible nitric oxide synthase in skeletal muscle involves AMPK but not SIRT1. *Am J Physiol Endocrinol Metab*. 2011;301:E922–E930. doi:10.1152/ajpendo.00530.2010
34. Alamdari N, Aversa Z, Castillero E, et al. Resveratrol prevents dexamethasone-induced expression of the muscle atrophy-related ubiquitin ligases atrogin-1 and MuRF1 in cultured myotubes through a SIRT1-dependent mechanism. *Biochem Biophys Res Commun*. 2012;417:528–533. doi:10.1016/j.bbrc.2011.11.154
35. Wang DT, Yin Y, Yang YJ, et al. Resveratrol prevents TNF-alpha-induced muscle atrophy via regulation of Akt/mTOR/FoxO1 signaling in C2C12 myotubes. *Int Immunopharmacol*. 2014;19:206–213. doi:10.1016/j.intimp.2014.02.002
36. Williams LD, Burdock GA, Edwards JA, Beck M, Bausch J. Safety studies conducted on high-purity trans-resveratrol in experimental animals. *Food Chem Toxicol*. 2009;47:2170–2182. doi:10.1016/j.fct.2009.06.002
37. Paschalaki KE, Starke RD, Hu Y, et al. Dysfunction of endothelial progenitor cells from smokers and chronic obstructive pulmonary disease patients due to increased DNA damage and senescence. *Stem Cells*. 2013;31:2813–2826. doi:10.1002/stem.1488
38. Hwang JW, Chung S, Sundar IK, et al. Cigarette smoke-induced autophagy is regulated by SIRT1-PARP-1-dependent mechanism: implication in pathogenesis of COPD. *Arch Biochem Biophys*. 2010;500:203–209. doi:10.1016/j.abb.2010.05.013